Electron Density. For a direct comparison of electron density in the monomer and polymeric fragments, we have computed two electron density maps, one being the central Be–H–B localized orbital of the trimer and the other being the Be–H–B localized orbital of the D_{2d} monomer, but with bond lengths constrained to equal those of the solid state. The trimer was chosen for computational convenience and because all indications are that electron reorganization upon going from the inner part of the trimer to the inner part of the hexamer is small compared to that from the monomer to the trimer (e.g., see Figures 5–7). The distortion of the monomeric D_{2d} bond lengths to those of the solid state allows a direct measure of reorganization of electron density brought about solely by BeB_2H_8 units bonding to each end of the monomer, and not by bond-length changes. In Figure 8, we show a difference electron density map calculated as

$$\rho_{\text{diff}} = \rho_{\text{trimer}} - \rho_{D_{2d}}$$

for the central Be–H–B localized orbital within the helix. The pronounced "flow" of electron density from the region of the beryllium to the region of the boron is another strong indication of the increased ionic character of the Be–B interaction within the helix.

Conclusion

Overlap populations, localized orbitals, and electron density comparisons all indicate that solid-state beryllium borohydride is best viewed as $BeBH_4^{\delta+}$–$BH_4^{\delta-}$, with the boron–beryllium interaction within the helix clearly being more ionic than in the D_{2d} monomer. This conclusion is consistent with the known geometrical parameters of the solid state[6] and the infrared spectrum of the solid.[7]

Calculated properties of the molecular wave function for the central region of the polymeric fragments show little difference between the pentamer and the hexamer. Therefore, it seems reasonable to conclude that the hexamer results are close to the limit of infinite chain length. Properties calculated from the center BeB_2H_8 unit of the trimer agree only moderately well with those calculated from the hexamer, but virtually all of the inaccuracies associated with the trimer properties are corrected at the pentamer level. The pentamer corresponds to two BeB_2H_8 units on each end of the central BeB_2H_8 moiety, and the above results indicate that two monomeric units are necessary to eliminate edge effects in modeling the solid-state polymer.

Acknowledgments. This work was partially supported by the Robert A. Welch Foundation.

References and Notes

(1) D. S. Marynick and W. N. Lipscomb, *J. Am. Chem. Soc.*, **95**, 7244 (1973).
(2) R. Ahlrich, *Chem. Phys. Lett.*, **19**, 174 (1973).
(3) D. S. Marynick, *J. Chem. Phys.*, **64**, 3080 (1976).
(4) M. J. S. Dewar and H. S. Rzepa, *J. Am. Chem. Soc.*, **100**, 777 (1978).
(5) (a) J. W. Nibler, *J. Am. Chem. Soc.*, **94**, 3349 (1972); (b) G. Gundersen, L. Hedberg, and K. Hedberg, *J. Chem. Phys.*, **59**, 3777 (1973).
(6) (a) D. S. Marynick and W. N. Lipscomb, *Inorg. Chem.*, **11**, 820 (1972); (b) *J. Am. Chem. Soc.*, **93**, 2322 (1971).
(7) J. W. Nibler, D. F. Shriver, and T. H. Cook, *J. Chem. Phys.*, **54**, 5257 (1971).
(8) A. B. Burg and H. I. Schlesinger, *J. Am. Chem. Soc.*, **62**, 3425 (1940).
(9) (a) J. W. Nibler and J. McNabb, *Chem. Commun.*, 134 (1969); (b) J. W. Nibler and T. Dyke, *J. Am. Chem. Soc.*, **92**, 2920 (1970).
(10) T. A. Halgren and W. N. Lipscomb, *J. Chem. Phys.*, **58**, 1596 (1973).
(11) C. E. Dykstra, H. F. Schaefar, and W. Meyer, *J. Chem. Phys.*, **65**, 5141 (1976), and references cited therein.
(12) T. A. Halgren, D. A. Kleier, J. H. Hall Jr., L. D. Brown, and W. N. Lipscomb, *J. Am. Chem. Soc.*, **100**, 6595 (1978).
(13) W. J. Hehre, R. F. Stewart, and J. A. Pople, *J. Chem. Phys.*, **51**, 2657 (1969).
(14) T. A. Halgren, R. J. Anderson, D. S. Jones, and W. N. Lipscomb, *Chem. Phys. Lett.*, **8**, 547 (1971).
(15) J. M. Foster and S. F. Boys, *Rev. Mod. Phys.*, **32**, 300 (1960).
(16) C. Edmiston and K. Ruedenberg, *Rev. Mod. Phys.*, **35**, 457 (1963).
(17) D. A. Dixon, I. M. Pepperberg, and W. N. Lipscomb, *J. Am. Chem. Soc.*, **96**, 1325 (1974).
(18) G. W. Mappes, S. A. Friedman, and T. P. Fehlner, *J. Phys. Chem.*, **74**, 3307 (1970).
(19) D. S. Marynick, J. H. Hall Jr., and W. N. Lipscomb, *J. Chem. Phys.*, **61**, 5460 (1975).
(20) I. R. Epstein, J. A. Tossell, E. Switkes, R. M. Stevens, and W. N. Lipscomb, *Inorg. Chem.*, **10**, 171 (1971).
(21) D. A. Kleier, T. A. Halgren, J. H. Hall Jr., and W. N. Lipscomb, *J. Chem. Phys.*, **61**, 3905 (1974).

X-ray Photoemission Study of Platinum Carbonyl Dianions $[Pt_3(CO)_6]_n^{2-}$ (n = 2, 3, 4, 5, 6, ~10)

G. Apai,* S.-T. Lee, M. G. Mason, L. J. Gerenser, and S. A. Gardner

Contribution from the Research Laboratories, Eastman Kodak Company, Rochester, New York 14650. *Received May 7, 1979*

Abstract: A series of platinum carbonyl dianion clusters has been studied by X-ray photoemission spectroscopy. Members of the series include $[Pt_3(CO)_6]_n^{2-}$ where n = 2, 3, 4, 5, 6, ~10. The general structure of all valence spectra, in particular that of the Pt 5d derived bands, is remarkably similar. This observation is taken to be evidence that negligible interaction exists between the $Pt_3(CO)_6$ layers. We observe changes in the binding energies of Pt 4f, Pt 4d, and the molecular orbitals ($5\sigma + 1\pi$) of the carbonyl ligands as a function of cluster size. All levels except the carbonyl 4σ orbitals are shifted to higher binding energy asymptotically as the cluster size increases. This behavior of binding energies is interpreted as being due to the decreasing effect of the anion charge in larger clusters and to the bonding character of the ($5\sigma + 1\pi$) orbitals.

Introduction

Metal cluster chemistry has become an additional way for surface-physics research to understand chemisorption of molecules on transition-metal surfaces. Recently, several papers have commented on the analogy which exists between transition-metal cluster complexes and few-atom bare metal clusters.[1] We and others feel that cluster complexes may provide a way of studying metal–metal and metal–adsorbate interactions in a more straightforward way than with metals themselves.

We have chosen to study platinum carbonyl dianion oligomers by X-ray photoemission spectroscopy (XPS) for several

0002-7863/79/1501-6880$01.00/0

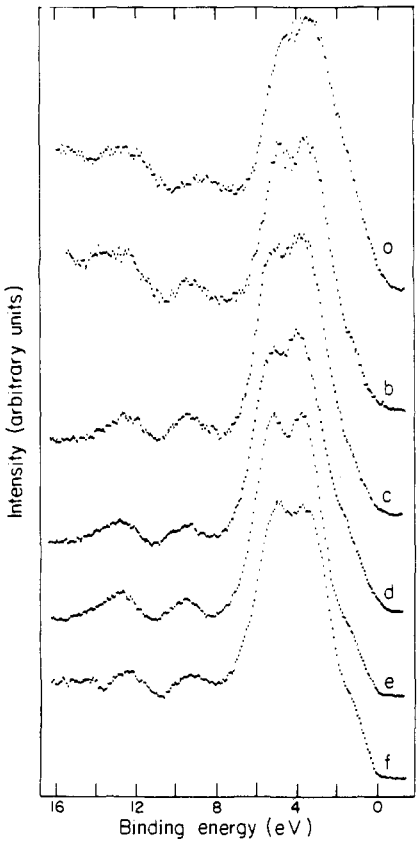

Figure 1. Valence XPS spectra of $[Pt_3(CO)_6]_n^{2-}$: (a) $n = 2$, (b) $n = 3$, (c) $n = 4$, (d) $n = 5$, (e) $n = 6$, and (f) $n \sim 10$.

reasons: (1) Small transition-metal carbonyl complexes may serve as models for chemisorption and catalysis by metal surfaces. (2) It is interesting both experimentally and theoretically to examine a uniform progression in the size of a transition-metal cluster which maintains a repeating geometric configuration. All of the clusters we have studied are composed of $Pt_3(CO)_6$ units stacked on top of each other. (3) XPS is unique in its ability to probe both the valence-band levels of a material and the core electronic levels. Also data are already available from XPS studies of small Pt clusters formed by vapor deposition.[2] (4) There is increasing evidence to show that carbonyl cluster complexes can be supported on oxide substrates and subsequently decarbonylated to yield bare metal clusters, presumably of the same size or slightly larger.[3]

Experimental Section

The series of dianions as tetra-*n*-butylammonium salts were prepared using the starting material sodium hexachloroplatinate (Alfa) in methanol solution. Our synthetic method, similar to that of Longoni and Chini,[4] resulted in progressive reduction of the platinum(IV) salt by carbon monoxide in the presence of alkali, where the size of the platinum oligomer was dependent on the alkali:Pt ratio. All reactions were run in a carbon monoxide atmosphere, using Schlenk-tube techniques. After each synthesis, the product was confirmed by characterizing the infrared absorptions in the carbonyl stretching region.

To minimize the contamination and possible decomposition of the samples by exposure to oxygen, the samples were prepared for XPS study in a dry nitrogen atmosphere in a glovebag. Typical preparation was to make a saturated solution of the platinum carbonyl in THF and deposit a thin uniform film of the liquid solution onto ultrapure graphite sheets, whose surface was then allowed to evaporate to dryness. The sample passed without exposure to air into a Hewlett-Packard 5950A electron spectrometer with a vacuum $\leq 1.0 \times 10^{-8}$ Torr. Spectra were taken at about 160 K to prevent possible decomposition within the vacuum and did not require the use of a sample-neutralizing electron-flood gun. Monochromatic Al $K\alpha_{1,2}$ radiation

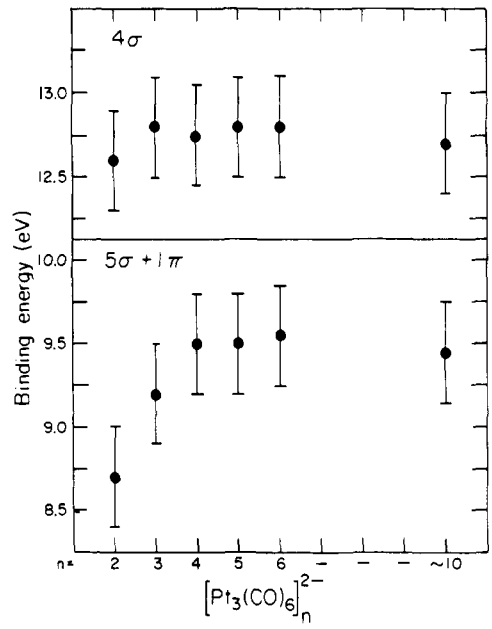

Figure 2. Variation in the binding energies for the 4σ and $(5\sigma + 1\pi)$ CO molecular orbitals as a function of platinum oligomer cluster size.

(1486.6 eV) was used for excitation, and the ejected photoelectrons were energy analyzed. The use of monochromatized X-rays reduces the minimum peak full width at half-maximum to ~0.6 eV and eliminates unwanted "bremsstrahlung" and X-ray satellite lines. For valence band (VB) spectra this is particularly useful.

Graphite substrates were chosen for two reasons: (1) Carbon has a VB which has a low photoemission cross section at Al $K\alpha$ X-ray energies and has only one core level which may overlap and interfere with other lines in the total spectrum. (2) Graphite is also a semimetal; consequently, charging the substrate and coated platinum carbonyl oligomers is not a problem, if the coating is thin enough.

In this study all core and valence-band binding energies (BE) have been referenced by the gold-evaporation technique.[5] Ginnard and Riggs have demonstrated that, by controlling the coverage of evaporated gold so each sample receives an equivalent amount, charges of ~5 eV or more on an insulating substrate may be corrected with a precision of better than ±0.2 eV. Graphite used in our study is a semimetal; however, the thin layer of Pt salt is nonconducting. Although no gross charging was apparent, requiring use of an electron-flood gun, careful control of evaporated gold was used for BE calibrations. After each sample was run, a number of Au evaporations were made with a core level analysis after each deposition. This provided a sequence of spectra which could be related to the increasing surface coverage of Au. Au 4f BE values were taken at coverages corresponding to surface electrically conductive coatings.

Results

Figure 1 shows valence-region XPS spectra of the $[Pt_3(CO)_6]_n^{2-}$ clusters. All spectra show remarkable resemblance. Each spectrum has an intense broad band in the 0–7-eV region, which can be attributed to the energy levels consisting predominantly of Pt 5d electrons. This "Pt band" in every spectrum is composed of a doublet separated by 1.3 ± 0.1 eV, with the lower binding energy component being slightly more intense. The doublet is resolved better in some cases than in others, which is traceable to sample inhomogeneity. Furthermore, the fwhm of the Pt band remains essentially unchanged at 4.0 ± 0.3 eV throughout the series. All spectra show two relatively weak bands at about 9 and 12.8 eV, which are primarily the $(5\sigma + 1\pi)$ and 4σ molecular orbitals of CO, respectively. The energy positions of these two bands vs. cluster size are plotted in Figure 2. The lower binding energy band moves to higher energy with increasing cluster size, approaching asymptotically to 9.5 eV at $n = 4$, whereas the energy position of the high-energy band stays essentially constant at 12.7 eV. The spectra did not show any distinguishable fea-

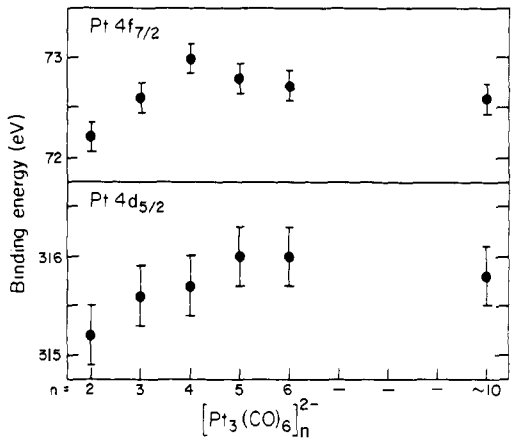

Figure 3. Variations in the core-level binding energies, Pt $4f_{7/2}$, and Pt $4d_{5/2}$ as a function of platinum oligomer cluster size.

ture which might be attributed to the two tetra-*n*-butylammonium cations. This is not at all surprising since the cross section of the butyl group is extremely small in the XPS region, and it is most likely lost in the rather intense background.

In addition to the valence levels, we have measured the BEs of the Pt 4f and Pt 4d core levels (Figure 3). All core-level BEs increase asymptotically with increasing cluster size and closely approach the asymptotic values at about $n = 5$.

Although precaution was taken in sample preparation, slight decomposition did occur in several samples. Such decomposition is conveniently detected in the 4f spectra by noting the presence of a shoulder on the low-energy side of the main Pt $4f_{7/2}$ peak. This is exemplified by comparing the Pt 4f spectra of $[Pt_3(CO)_6]_3^{2-}$ and $[Pt_3(CO)_6]_5^{2-}$ in Figure 4, where the latter shows a definite low-energy shoulder.

From the energy position of the shoulder, i.e., ~71 eV, the decomposed product is tentatively identified as Pt metal, and the valence band of Pt should contribute to the intensity near the threshold of the cluster valence spectra. This assignment is consistent with the observation that a more intense Pt 4f shoulder is accompanied by higher intensity at the threshold of the valence spectra (Figures 1 and 4). Using this characteristic, we detected noticeable decomposition in clusters $n = 5$, 6, and 10. Some slight decomposition to other members of the series may have evaded detection. Other than the presence of the low-energy shoulder, all Pt 4f peaks appeared quite symmetric with their fwhm varying between 1.4 and 1.8 eV, reflecting primarily the differential charging due to sample inhomogeneity.

Discussion

In spite of the dianionic character of the Pt clusters, their valence XPS spectra are qualitatively similar to those of neutral transition-metal carbonyls.[6,7] Like those of the neutral carbonyls, the valence spectra can be conveniently assigned in terms of Pt and CO derived bands. Therefore, the strong first energy band falling between 0 and 7 eV is assigned to the Pt 5d levels, the second band at ~9 eV to CO ($5\sigma + 1\pi$) MOs, and the third band at ~12.7 eV to CO 4σ MOs. This assignment is consistent with the normally weak bonding interaction between the ligand and metal orbitals, such that they undergo little change upon cluster formation. However, there are three interesting features unique to the Pt clusters themselves: (1) The Pt band is insensitive to the size of the cluster. All Pt bands show a similar band profile and exhibit a doublet with 1.3-eV separation and fwhm of ~4 eV. (2) The ratio of CO intensity to Pt band intensity is unusually low. Using the CO/metal band intensity ratio found in some polynuclear carbonyls[8] and the calculated cross sections of the metal valence d orbitals,[9] we expect the CO/Pt band intensity ratio to be ~1/7. The experimental values vary between 1/12 and 1/21, and are thus a factor of ~2 too low. (3) Different behavior of the BEs of CO ($5\sigma + 1\pi$) and 4σ bands is observed as a function of cluster size (Figure 2).

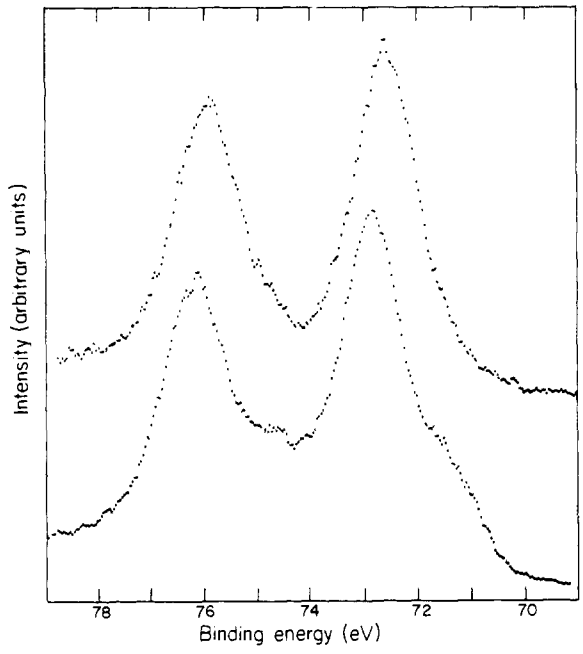

Figure 4. Comparison of Pt 4f spectra for $[Pt_3(CO)_6]_3^{2-}$ (top) and $[Pt_3(CO)_6]_5^{2-}$ (bottom). The presence of some decomposition is noticeable in the spectrum for $[Pt_3(CO)_6]_5^{2-}$ which is attributed to Pt metal.

The logical deduction which can be drawn from the similarity of the Pt bands is that the bonding interaction between $Pt_3(CO)_6$ layers is small. This weak interaction is not surprising in view of the relatively long intertriangular Pt–Pt distance between $Pt_3(CO)_6$ units along the pseudo-threefold axis.[10] Furthermore, recent Pt NMR results[11] on $[Pt_3(CO)_6]_3^{2-}$ which show fluxional behavior of the outer Pt_3 triangles with respect to the middle triangle are consistent with this assertion. Therefore, to a good approximation, the electronic structure of the Pt clusters can be treated as the $Pt_3(CO)_6$ unit but with proper allowance made for the dianion charge. Owing to the lack of reliable calculations, analysis of the Pt band has to be qualitative. The general structure of the Pt XPS band leads us to postulate that the electronic structure of $Pt_3(CO)_6$ can be compared to that of a single Pt atom of $5d^{10}$ configuration in the presence of other Pt and CO ligands. This is reasonable because the strong spin–orbit interaction in Pt is likely to be more important than the ligand field effects. In this picture, the Pt band can be interpreted as the spin–orbit doublet of Pt 5d orbitals, and the broadening of the individual doublet components is then the result of ligand field splitting, lifetime broadening, and of course inhomogeneous sample charging. The 1.3-eV separation in the Pt band compares well with the 1.1-eV spin–orbit splitting of free Pt 5d electrons.[12] The excess charge introduced by the anionic character would go into the Pt 6s orbital. The latter has very low cross section in the XPS energy region and thus has little effect on the band and our interpretation. If our postulate is correct, we would expect the Pt band of the clusters to closely approximate the spectrum of supported Pt nuclei consisting of either single or a few atoms with $5d^{10}$ configurations. Unfortunately, since the small Pt nuclei supported on carbon exist essentially in the $5d^96s^1$ configuration,[2] a meaningful comparison of their XPS spectra is not feasible, owing to multiplet structure. However, we found that small supported Au nuclei existed in the $5d^{10}6s^1$ configuration.[13] Comparing the spectra of small Au nuclei and the

Pt clusters, we found, as expected, a close similarity (except of course for the difference in the spin–orbit splitting, which is 1.8 eV for Au). This agreement offers support for our postulate and serves to link the study of metal clusters to that of catalytic metal nuclei.

One reason for the low CO/Pt intensity ratio is the loss of CO due to decomposition to metallic Pt. This finds support in that the ratio is generally lower in the larger clusters which, as shown earlier, noticeably decomposed. Yet, even after allowance is given for this cause, the ratio is still at least a factor of 1.5 too low. This may result from two possible causes—intrinsic loss processes such as shakeup[14] or molecular orbital dilation resulting from the excess negative charge on the CO moiety.

The binding energy of the CO molecular orbitals is also influenced by the excess negative charge. In metal carbonyls[15] the terminal and bridging carbonyls are bonded to the metal mainly through 5σ and 1π MOs of CO, whereas the O lone pair (4σ MO) remains essentially nonbonding or slightly antibonding. Therefore, it is expected that ($5\sigma + 1\pi$) derived MOs which are involved in bonding in the clusters are more sensitive to the perturbation of cluster formation. Furthermore, whatever portion of the two negative charges that goes into the CO moieties probably occupies the antibonding CO 2π MOs. Since this orbital is primarily C 2p in character, the negative charge is highly localized on carbon.[16] As a result, 5σ and 1π MOs which have a significant carbon contribution[16] should be more susceptible to the amount of negative charge on the $Pt_3(CO)_6$ unit than the 4σ MO. The different behavior of the BEs of ($5\sigma + 1\pi$) and 4σ derived bands is attributable to their respective bonding and nonbonding character. The asymptotic increase of the ($5\sigma + 1\pi$) BE with increasing cluster size is accountable then by the decreasing negative charge per $Pt_3(CO)_6$ unit. The increasing BE trend agrees with the IR data[4] giving an increase in absorption frequency, thus stronger bonding for the terminal CO groups with increasing cluster size.

Binding energy of core levels is also closely related to local charge. Since negative charges on Pt atoms decrease for larger clusters, it is expected that the BEs of Pt 4f and 4d should increase with increasing cluster size. The variations in Pt core level BE with cluster size (Figure 3) can qualitatively be explained in terms of a simple spherical charge model.[17] In the present cluster case this model is practically the same as the more elaborate and successful potential model.[17] This is because of the negligible interlayer interaction, such that molecular potential and relaxation energy can be regarded as the same throughout the series. In the spherical charge model, the binding energy shift ΔE is proportional to q/r, where q is the atomic charge and r is the atomic radius. Using the Bohr model of atoms, r is proportional to $1/q$, and, since q is inversely proportional to n, this results in $\Delta E \propto 1/n^2$. This variation of BE shift, as the inverse of n^2, then explains the observed shape of the asymptotic curves shown in Figure 3.

The absolute BEs of the Pt 4f's and 4d's are appreciably larger than the corresponding values for bulk Pt metal ($4f_{7/2}$ BE = 71.0 eV and $4d_{5/2}$ BE = 314.8 eV).[2] In fact, the Pt $4f_{7/2}$ BEs here are closer to those found in PtO, which is 73.4 eV,[19] than to that in Pt metal. This anomalous behavior is thought to result from two factors. First, photoemission[20] and work function[21] measurements indicate that CO withdraws electrons when adsorbed on Pt metal. Theoretical calculations for Ni also show significant electron transfer away from the transition metal upon CO adsorption.[22] The residual positive charge on Pt should produce a shift to higher binding energy, as observed. In fact, it is generally true that metal carbonyls show core-level binding energies which are higher than those observed in the bulk metals.[7,18] The same should hold for the ionic clusters of large n where the anionic charge is dispersed over many atoms. The second factor which contributes to the high metal binding energy in metal carbonyls is the incomplete extraatomic relaxation. As mentioned earlier, there is very little interaction between adjacent $Pt_3(CO)_6$ groups. The extraatomic relaxation is therefore diminished in comparison to the bulk metal, and the core-level binding energies are accordingly higher.

Conclusions

The XPS study of the series $[Pt_3(CO)_6]_n^{2-}$ presents a unique example by which a correlation between BE shift and charge is demonstrated directly by experiment. Thus, the core-level BE shift follows roughly a $1/n^2$ dependence of the anionic charge. From the analysis of the valence spectra, we are led to believe that interlayer interactions are small so that the electronic structure of the series is basically like that of a single $Pt_3(CO)_6$ unit with the appropriate charge. Furthermore, because of the strong spin–orbit coupling of Pt 5d electrons, the Pt valence spectra of the clusters can be understood satisfactorily in terms of a single Pt atom of $5d^{10}$ configuration perturbed by ligand fields. By analogy, we believe that, in favorable cases, the metal carbonyl clusters could serve as model systems for the study of catalytic metal nuclei having the same valence electron configuration.

References and Notes

(1) Muetterties, E. L. *Science* **1977**, *196*, 839. Smith, A. K.; Basset, J. M. *J. Mol. Catal.* **1977**, *2*, 229. Conrad, H.; Ertl, G.; Knözinger, H.; Küppers, J.; Latta, E. E. *Chem. Phys. Lett.* **1976**, *42*, 115.
(2) Mason, M. G.; Gerenser, L. J.; Lee, S.-T. *Phys. Rev. Lett.* **1977**, *39*, 288.
(3) Smith, G. C.; Chojnacki, T. P.; Dasgupta, S. R.; Iwatate, K.; Watters, K. L. *Inorg. Chem.* **1975**, *14*, 1419. Ichikawa, M. *J. Chem. Soc., Chem. Commun.* **1976**, *11*. Gallezot, P.; Coudurier, G.; Primet, M.; Imelik, B. "Molecular Sieves II", Katzer, J. R., Ed.; ACS Symposium Series No. 40, American Chemical Society: Washington, D.C., 1977; p 144.
(4) Longoni, G.; Chini, P. *J. Am. Chem. Soc.* **1976**, *98*, 7225.
(5) Ginnard, C. R.; Riggs, W. M. *Anal. Chem.* **1974**, *46*, 1306.
(6) Higginson, B. R.; Lloyd, D. R.; Burroughs, P.; Gibson, D. M.; Orchard, A. F. *J. Chem. Soc., Faraday Trans. 2* **1973**, *69*, 1659.
(7) Salaneck, W. R., private communication.
(8) Lee, S.-T.; Mason, M. G., unpublished. Valence XPS spectra of $Ir_4(CO)_{12}$, $Ru_3(CO)_{12}$, $Os_3(CO)_{12}$, and $Rh_6(CO)_{16}$ were used in the estimation.
(9) Scofield, J. H. S. *J. Electron Spectrosc. Relat. Phenom.* **1976**, *8*, 129.
(10) Calabrese, J. C.; Dahl, L. F.; Chini, P.; Longoni, G.; Martinengo, S. *J. Am. Chem. Soc.* **1974**, *96*, 2614.
(11) Brown, C.; Heaton, B. T.; Chini, P.; Fumegalli, A.; Longoni, G. *J. Chem. Soc., Chem. Commun.* **1977**, 309.
(12) Moore, C. E. "Atomic Energy Levels as Derived from Analysis of Optical Data", NBS Data Series No. 35: Washington, D.C., 1971.
(13) Lee, S.-T.; Apai, G.; Mason, M. G.; Hurych, Z.; Benbow, R., to be submitted for publication.
(14) Plummer, E. W.; Salaneck, W. R.; Miller, J. S. *Phys. Rev. B* **1978**, *18*, 1673.
(15) Cotton, F. A.; Wilkinson, G. "Advanced Inorganic Chemistry", 2nd ed.; Interscience: New York, 1966.
(16) Snyder, L. C.; Basch, H. "Molecular Wave Functions and Properties"; Wiley: New York, 1972.
(17) Siegbahn, K., et al. "ESCA Applied to Free Molecules"; Elsevier: New York, 1969.
(18) Barber, M.; Connor, J. A.; Guest, M. F.; Hall, M. B.; Hillier, I. H.; Meredith, W. N. E. *Faraday Discuss. Chem. Soc.* **1972**, *72*, 219.
(19) Kim, K. S.; Winograd, N.; Davis, R. E. *J. Am. Chem. Soc.* **1971**, *93*, 6296.
(20) Apai, G.; Wehner, P. S.; Stöhr, J.; Williams, R. S.; Shirley, D. A. *Solid State Commun.* **1976**, *20*, 1141.
(21) Morgan, A. E.; Somorjai, G. A. *J. Chem. Phys.* **1969**, *51*, 3309.
(22) Bullett, D. W.; Cohen, M. L. *Solid State Commun.* **1977**, *21*, 157.